Microchemical Journal xxx (xxxx) 109890

Contents lists available at ScienceDirect

Microchemical Journal

journal homepage: www.elsevier.com/locate/microc

Molecularly imprinted polypyrrole-based electrochemical melamine sensors

Ernestas Brazys [a], Vilma Ratautaite [b, c, *], Benediktas Brasiunas [c], Almira Ramanaviciene [c], Laura Rodríguez [d, e], Andrea Pinto [d, e], Demetrio Milea [f], Urte Prentice [a, b], Arunas Ramanavicius [a, b, *]

[a] Department of Physical Chemistry, Institute of Chemistry, Faculty of Chemistry and Geosciences, Vilnius University (VU), Naugarduko str. 24, Vilnius LT-03225, Lithuania
[b] Department of Nanotechnology, State Research Institute Center for Physical Sciences and Technology (FTMC), Sauletekio Ave. 3, Vilnius LT-10257, Lithuania
[c] NanoTechnas – Center of Nanotechnology and Materials Science, Institute of Chemistry, Faculty of Chemistry and Geosciences, Vilnius University (VU), Naugarduko str. 24, LT-03225 Vilnius, Lithuania
[d] Departament de Química Inorgànica i Orgànica, Secció de Química Inorgànica, Universitat de Barcelona, Martí i Franquès 1-11, 08028 Barcelona, Spain
[e] Institut de Nanociència i Nanotecnologia (IN2UB), Universitat de Barcelona, 08028 Barcelona, Spain
[f] Dipartimento di Scienze Chimiche, Biologiche, Farmaceutiche ed Ambientali, CHIBIOFARAM, Università degli Studi di Messina, V. le F. Stagno d'Alcontres, 31, I-98166 Messina, Italy

ARTICLE INFO

Keywords:
Molecularly imprinted polymer (MIP)
Polypyrrole (Ppy)
Melamine
Electrochemical sensor
Gold nanoparticles (AuNPs)
Gold(I) complexes

ABSTRACT

This study describes the development of a molecularly imprinted polymer (MIP) polypyrrole-based (Ppy-based) electrochemical melamine sensor. Two different modifications of polymeric layers in the design of MIP-based melamine sensor systems were assessed. The addition of gold nanoparticles (AuNPs) or gold(I) complexes in the polymerization solution containing pyrrole was studied. The characteristics of all polypyrrole layers were evaluated indirectly using a $[Fe(CN)_6]^{3-}/[Fe(CN)_6]^{4-}$ as a redox probe by application of differential pulse voltammetry (DPV). The most optimal results were obtained when the MIP polymerization was prepared from a solution containing 50 mM pyrrole, 5 mM melamine, and 0.05 nM 3.5 nm diameter AuNPs. Under these conditions, the observed response of MIP to melamine was 6.61 times greater than that of non-imprinted polymer (NIP). To further characterize the detection of melamine, overoxidized forms of both MIP and NIP were employed. The utilization of MIP resulted in a linear correlation within the concentration range from 50 nM to 5 μM melamine, with an estimated limit of detection (LOD) of 0.83 nM melamine.

1. Introduction

Melamine is a compound commonly used in the plastics industry to produce melamine–formaldehyde resins. It contains a significant amount of nitrogen (66 % by mass), which has led to its misuse by unethical manufacturers who add it to dairy products to avariciously inflate measured protein levels. The consumption of melamine caused harmful effects that gained worldwide attention during the 2007 pet food outbreak in North America. Throughout this outbreak, numerous cases of acute renal failure in house pets, dogs and cats, were linked to melamine-contaminated pet foods. Another notorious incident occurred in 2008 when melamine-contaminated milk caused urinary stones in children under the age of 3 in China [1,2]. It was determined that melamine is nephrotoxic to humans and the consumption of this compound can cause renal diseases [3]. The European Community, the US Foods and Drug Administration, and other responsible authorities, and institutions have defined limits for melamine in numerous food products. The concentration of melamine is restricted to 1 ppm in baby formula and 2.5 ppm in other dairy products [4]. Consequently, reliable methods for melamine determination are necessary to enforce these regulations. A wide range of techniques has been developed to detect melamine. Some of these methods have been reviewed and summarized by Lu et al., [5]. Instrumental analysis methods, such as gas chromatography and liquid chromatography, offer high accuracy and sensitivity. However, these techniques are limited by the necessity of expensive equipment, difficult operation, and long analysis duration, thus making the application of these methods in the milk industry less appealing. In contrast, sensor-based analytical techniques have an advantage over instrumental analysis methods because they are cheaper and faster, and the analysis can be performed by untrained personnel. Naturally, these more budget-friendly alternatives are being recognized for their ability to detect melamine molecules. The study of Cao et al., [6]

* Corresponding authors.
E-mail addresses: ernestas.brazys@chgf.vu.lt (E. Brazys), vilma.ratautaite@ftmc.lt (V. Ratautaite), benediktas.brasiunas@chgf.vu.lt (B. Brasiunas), almira.ramanaviciene@chf.vu.lt (A. Ramanaviciene), laurarodriguezr@ub.edu (L. Rodríguez), andrea.pinto@qi.ub.es (A. Pinto), dmilea@unime.it (D. Milea), urte.prentice@ftmc.lt (U. Prentice), arunas.ramanavicius@chf.vu.lt (A. Ramanavicius).

https://doi.org/10.1016/j.microc.2024.109890
Received 1 September 2023; Received in revised form 14 December 2023; Accepted 1 January 2024

reports a chemosensor that detects melamine based on the hydrogen bonding interactions between melamine and the AuNPs-modified sensor surface. The researchers have developed a colorimetry method utilizing a label-free AuNP assay for the identification of melamine. AuNPs were prepared using 3,5-dihydroxybenzoic acid as a reducer. The presence of melamine inhibits the formation of these nanoparticles as the melamine tends to interact with 3,5-dihydroxybenzoic acid through hydrogen-bonding interactions. This leads to an insufficient amount of a reducer for the reduction of Au^{3+} ion, resulting in the color change from purple to yellow-green with the increase of melamine concentration. Zhao et al., [7] employed 3,4-dihydroxyphenylacetic acid for electrochemical sensor development. In this study, melamine was reported to form complexes with 3,4-dihydroxyphenylacetic acid *via* hydrogen bonds.

MIP can also be applied to develop melamine sensing systems [5, 8–12]. MIPs are synthetic polymers that mimic the antibody function to affinity interact with the corresponding antigen. MIP selectively interacts with the molecules, which were denoted as the template during the polymerization [13]. MIP can possess the advantages of antibody-antigen interaction such as high specificity and selectivity along with resistance to environmental conditions and cheap production [14–16]. Optimal storage and application conditions are necessary for immobilized antibody or antigen. On the contrary, MIP-based systems can technically be preserved indefinitely, as they typically do not require any special care. Furthermore, MIP can be implemented over a broader temperature interval [14–16]. The production of MIP generally follows the same principle: (i) monomers and template molecules are mixed in the solution and allowed to self-assemble; (ii) a polymer is produced from a bulk solution containing the template molecules, that bind either covalently or non-covalently to functional groups of the monomers during the self-assembly process, (iii) the template molecules are then extracted from the polymeric layer while retaining template-specific cavities available for rebinding processes, and (iv) the MIP is then exposed to the template-containing sample, therefore the cavity selectively rebinds with the template molecule from a sample [10].

MIP can be incorporated with a variety of compounds, including nanomaterials, for the improvement of the sensor's characteristics. Graphene-AuNPs were applied to enhance the properties of Ppy-based MIP in the study by Wang et al., [9]. In this study, an electrochemical levofloxacin sensor was developed. The authors state that graphene-AuNPs significantly improved the oxidation of levofloxacin, therefore, the sensitivity has increased. Essousi et al., [17] study describes a reduced graphene oxide and Ppy composite-based MIP which they overoxidized in 0.1 M NaOH solution using cyclic voltammetry (CV) in the potential range from + 0.1 V to + 1 V *vs* $Ag/AgCl_{(3M\ KCl)}$. Overoxidized Ppy-based MIP with reduced graphene oxide was later incorporated with AuNPs to increase conductivity. This sensor was applied in the determination of amoxicillin and it features high reproducibility, good stability, and selectivity. Gu et al., [18] reported a study about overoxidized Ppy-AuNPs composite-based MIP in the design of an electrochemical sensor dedicated to cysteine enantiomers recognition. The researchers have incorporated polymers with AuNPs to take advantage of the Au-S bonding. The sensitivity and selectivity of the overoxidized Ppy-AuNPs composite-based MIP are superior to non-modified MIP in the recognition of cysteine enantiomers. The modification with different nanostructures serves different purposes. The implementation of AuNPs to Ppy composites can exhibit higher sensitivity to target analyte molecules due to their electrocatalytic properties and increased hydrogen bonding [19–21]. Yu et al., [22] reported a specific electrochemical melamine sensor utilizing an aptamer and AuNPs. The authors incorporated polydopamine-based MIP and melamine binding DNA aptamers (5′-SH-TTTTTT-3′) in this research. AuNPs were produced by reducing with sodium citrate followed by the modification of the glassy carbon electrode (GCE) with AuNPs. Afterwards, modified AuNPs/GCE electrode was immersed in an aptamer-melamine composite mixture to form aptamer-melamine/AuNPs/GCE. Then, MIPs were formed by electropolymerization of dopamine by cycling the potential from –0.5 V to + 1.0 V. Polymerization of dopamine was carried out from a solution containing dopamine and polythymine in the presence of melamine as a template. Electrochemical analysis was performed with a commonly used redox probe of 5 mM $K_3[Fe(CN)_6]/K_4[Fe(CN)_6]$ and CV and differential pulse voltammetry (DPV). This electrochemical MIP-aptamer sensor displayed a linear relationship between 10^{-12} M and 10^{-4} M for detecting melamine using DPV with the limit of detection (LOD) of 6.7×10^{-13} M. Another MIP-based electrochemical sensor has been described by Regasa et al., [23]. In this paper, the polymer composite was co-electropolymerized from a mixture consisting of aniline and acrylic acid as monomers and melamine serving as the template. The characterization of this sensor was carried out similarly to the previous study – by DPV using a ferri/ferrocyanide redox pair and the linearity was from 0.1 nM to 180 nM of melamine, and the LOD was 0.0172 nM. One of the earlier attempts to develop a MIP-based sensor for melamine detection was reported by Liang et al., [24] study. In the aforementioned study, methacrylic acid was chosen as a functional monomer and polymerized chemically in the presence of melamine. The membrane electrodes were prepared from the obtained MIP and NIP and detected protonated melamine using potentiometric analysis. As it was reported in that study, melamine tended to protonate at a pH lower than 5.0. Liang et al., [24] study reported that the MIP-based membrane electrode displayed a near-Nernstian signal in the melamine concentration interval from 5.0×10^{-6} to 1.0×10^{-2} M. The sensor possessed high stability and rapid response to the analyte. A melamine sensor based on MIP was presented by Wu et al., [25]. In keeping with standard practice, the monomer 2-mercapto benzimidazole was subjected to polymerization in the presence of the template molecule melamine. In this particular instance, electrochemical initiation utilizing CV was employed for the polymerization process. The electrochemical signal was monitored using a redox probe (5 mM $[Fe(CN)_6]^{3-}/[Fe(CN)_6]^{4-}$) and CV and electrochemical impedance spectroscopy (EIS). Wu et al., [25] fitted EIS data using R(Q(RW)) (Randles) circuit and the calibration curve was constructed using estimated charge transfer resistance R_{ct}. LOD from calibration plot R_{ct} *vs* melamine concentration in this study was as low as 3.0×10^{-9} M and stated that the developed method can be adapted to detect other non-electrochemically active molecules in food samples in the future. An electrochemical sensor based on melamine imprinted poly(*para*-aminobenzoic acid) was developed by Liu et al., [26]. In this study the signal was determined using 2 mM $[Fe(CN)_6]^{3-}/[Fe(CN)_6]^{4-}$ redox couple and CV, EIS, and DPV methods. Using DPV the authors observed a linear correlation in the melamine concentration range from 4.0×10^{-6} M to 4.5×10^{-4} M with LOD of 0.36 μM. This research demonstrated another methodology example for the detection of the electrochemically inactive analyte based on the MIP technique.

In the present work, the development of MIP Ppy-based electrochemical melamine sensors is described. The sensors were also further modified by incorporating either different-size AuNPs or gold(I) complexes. The novelty of this article is based on the application of the aforementioned materials in the fabrication process of the sensors for melamine detection.

2. Materials and methods

2.1. Chemicals and instrumentation

Pyrrole (CAS: 109–97-7) was acquired from Alfa Aesar (Kandel, Germany) and was subjected to distillation before its utilization. All other chemical reagents were of an analytical grade and were used in the experiments as obtained. Potassium chloride (CAS: 7447–40-7), potassium hexacyanoferrate (III) (CAS: 13746–66-2), tannic acid (CAS: 1401–55-4), and trisodium citrate (CAS: 68–04-2) were acquired from

Carl Roth (Karlsruhe, Germany). Sodium dihydrogen phosphate (CAS: 10049–21-5), disodium hydrogen phosphate (CAS: 7558–79-4), hydrochloric acid (CAS: 7647–01-0), sodium hydroxide (CAS: 1310–73-2), and melamine (CAS: 108–78-1) were purchased from Alfa Aesar (Kandel, Germany), while sodium carbonate (CAS: 497–19-8) and sulfuric acid (96 %) (CAS: 7664–93-9) from Lachner (Neratovice, Czech Republic). Ethanol (CAS: 64–17-5) was purchased from Riedel-de Haën (Seelze, Germany), and potassium hexacyanoferrate(II) (CAS: 14459–95-1) from Reachim (Donetsk, Ukraine). Imidazole (>99.5 %) (CAS: 288–32-4) and iodoethane (99 %) (CAS: 75–03-6) were purchased from Sigma-Aldrich (Steinheim, Germany). 1H-benzo[d] imidazole (CAS: 51–17-2) and 9,10-phenanthrenequinone (CAS: 84–11-7) were purchased from Fluorochem (Hadfield, UK). Silver(I) oxide (99 %) (CAS: 20667–12-3) was purchased from Alfa Aesar (Kandel, Germany). Hydrogen tetrachloroaurate(III) trihydrate (CAS: 16961–25-4) was purchased from Sigma-Aldrich (Steinheim, Germany).

Infrared spectra have been recorded on an FT-IR 520 Nicolet Spectrophotometer. 1H NMR (δ(TMS) = 0.0 ppm) spectra have been recorded on a Varian Mercury 400 and Bruker 400. ElectroSpray-Mass spectra (+) have been recorded on a Fisons VG Quatro spectrometer.

All electrochemical polymerization and electrochemical analysis of polymer experiments were performed in phosphate-buffered saline (PBS) based solutions. PBS solution consisted of 10 mM disodium hydrogen phosphate and 1.8 mM sodium dihydrogen phosphate. The ionic strength of PBS was supported with 0.1 M KCl. The pH value of the PBS solution was altered to 7.40 with 0.1 M HCl – the changes in pH were monitored using pH-meter SevenCompact S220 (Greifensee, Switzerland).

All electrochemical measurements were performed with a computer-controlled potentiostat/galvanostat Methrohm Autolab μAutolabIII/FRA2 μ3AUT71079 equipped with NOVA 2.1.3 software from EcoChemie (Utrecht, The Netherlands). A three-electrode system was applied for all electrochemical measurements and consisted of $Ag/AgCl_{(3M\ KCl)}$ as the reference electrode, a platinum wire as the counter electrode, which both were purchased from ItalSens (Houten, The Netherlands). A graphite rod with a diameter of 3 mm, obtained from Sigma-Aldrich (St. Louis, USA), was employed as the working electrode. Hitachi SU70 scanning electron microscope (SEM) was used to study the surface morphology of the films.

2.2. Pretreatment of the working electrode

The graphite rod was prepared as previously reported [27] – the surface was sequentially treated with 200, 900, and 2000 grit sandpaper. It was followed by polishing the electrodes with a sheet of paper, resulting in a smooth electrode surface. Furthermore, the graphite rod electrodes were rinsed with acetone and deionized water, and then the sides of the electrodes were covered with a silicone tube to avoid the electrode side contact with the solution. Finally, the working electrode was treated electrochemically in 10 mM PBS solution, pH 7.4 by CV in the potential range from –1.0 V to + 1.0 V *vs* $Ag/AgCl_{(3M\ KCl)}$, at the sweep rate of 100 mV s^{-1} and step potential of 2.44 mV, until a stable baseline was attained (10 potential cycles).

2.3. Preparation of AuNPs and gold(I) complexes

AuNPs of 3.5 nm, 6 nm, and 13 nm diameters were synthesized as described in the previously published paper [28]. A 40 mL aqueous solution of hydrogen tetrachloroaurate (0.01 % [w/v]) was heated to 60 °C. Secondly, another 10 mL solution containing sodium citrate (0.2 % [w/v]) and different concentrations of tannic acid (0.25 % [w/v] for 3.5 nm AuNPs, 0.025 % [w/v] – 6 nm, 0.00125 % [w/v] – 13 nm) was heated to 60 °C and added to hydrogen tetrachloroaurate solution under vigorous stirring. The mixture was then heated to 95 °C and held at that temperature for 5 min. Additionally, for 3.5 nm AuNPs synthesis, at this point, 2.5 mL of 25 mM Na_2CO_3 was added to neutralize the acidic pH of the synthesis solution. All synthesis solutions were then allowed to cool to room temperature. Before use, AuNPs were stored at + 4 °C.

Gold(I) complexes (**1**–**3**) were synthesized according to previously published methods [29]. They were produced by reacting the corresponding previously synthesized imidazole salt with Ag_2O, followed by a ligand exchange reaction with [AuCl(tht)] and recrystallization with dichloromethane/hexane. The structural formulas of the gold(I) complexes used in this research are presented in Fig. 1.

2.4. Electrochemical deposition of MIP and NIP layers

First, the polymerization solution composition optimization experiments were carried out. MIP was synthesized from a 10 mL mixture consisting of 50 mM pyrrole as a monomer and 5 mM melamine as template molecules. AuNPs or gold(I) complexes were added to the polymerization solution to increase the electrocatalytic properties of polymer layers. The exact materials and their concentrations used to modify polymers are presented in Table 1.

Before conducting the synthesis of MIP, the polymerization mixture was prepared and left for 1 h for self-assembly processes to occur. MIPs on the electrode were formed electrochemically by a series of 20 potential pulses of + 1.0 V *vs* $Ag/AgCl_{(3M\ KCl)}$ for 2 s, between each of the pulses 0 V potential pulse for 10 s was applied. The template molecules from formed MIP were extracted by immersing layers in 1 M sulfuric acid solution and stirring for 1 h at 300 rpm. As reference layers, NIPs were produced according to the same process but in the absence of melamine molecules. To reduce differences between polymeric layers, NIP was also exposed to a 1 M sulfuric acid solution.

2.5. Sensor signal evaluation

Melamine presence was assessed using a 5 mM $K_3[Fe(CN)_6]/K_4[Fe(CN)_6]$ redox probe. Prepared MIP layers were incubated in PBS solution without melamine for 10 min. The characteristics of MIP layers were monitored using the DPV when the step potential was 5 mV, modulation amplitude 25 mV, modulation time 50 ms, and interval time 500 ms. DPV was carried out in the potential range from 0 V to + 0.6 V *vs* $Ag/AgCl_{(3M\ KCl)}$. Then, following the same procedure, the imprinted layer was incubated in the PBS solution with 1 μM of melamine. After incubation, the working electrodes were washed under a stream of deionized water to wash away the non-

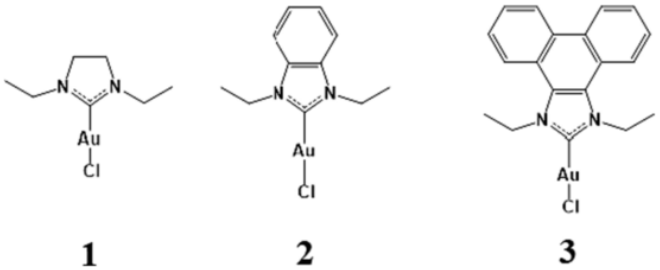

Fig. 1. The structural formulas of the gold(I) complexes (**1**–**3**).

Table 1
Materials and their concentrations used to modify polymers.

Material	Concentration
3.5 nm diameter AuNPs	0.01 nM; 0.05 nM or 0.1 nM
6 nm diameter AuNPs	0.01 nM; 0.05 nM or 0.1 nM
13 nm diameter AuNPs	0.01 nM; 0.05 nM or 0.1 nM
Gold(I) complex (1)	1.0 μM
Gold(I) complex (2)	1.0 μM
Gold(I) complex (3)	1.0 μM

specifically bound analyte. The layer with bound melamine was once again monitored by DPV. NIP was evaluated according to the same protocol.

3. Results and discussions

Two types of Ppy layers, MIP and NIP, were electrochemically prepared on the surface of the graphite rod electrode. Polymerization solution contained 50 mM pyrrole and 5 mM melamine for the deposition of MIP, and 50 mM pyrrole for the deposition of NIP. Polymerization of pyrrole was expected to take place during the pulses at a potential value of + 1.0 V. The final MIP and NIP structure was formed only after the template extraction step. Hence, the entrapped melamine templates were extracted from the formed Ppy layer during the next MIP production step. To accomplish this, the formed MIP layer was immersed in a 1 M H_2SO_4 solution while stirring for 1 h at 300 rpm. Analogously, the NIP layer was also exposed to a 1 M H_2SO_4 solution to minimize the differences between the two layers caused by the extraction procedure. Subsequently, the electrodes with MIP and NIP layers were assessed electrochemically. DPV curves of the MIP and the method of extracting the analytic signal from raw DPV data are presented in Fig. 2A. Both MIP and NIP demonstrated the decrease of oxidation peak current after the incubation in a PBS solution with 1 μM melamine. This decrease in the current value can be explained by the hindrance of electron pathways due to the interactions of the film with the melamine [30]. In this case, MIP interacted with melamine specifically and non-specifically. In contrast, NIP exhibited solely non-specific interactions with melamine [31]. To convey the differences in the interaction with template molecules more clearly, a relative decrease in the current ($\Delta I_{\%}$) after the incubation process was calculated according to equation (1):

$$\Delta I_{\%} = -\left(\frac{I_{pa1} - I_{pa0}}{I_{pa0}}\right) \times 100\,\% \quad (1)$$

where I_{pa1} – peak oxidation current after incubation in PBS with 1 μM melamine, in μA; I_{pa0} – peak oxidation current after incubation in PBS with no melamine, in μA.

One of the methods to determine the quality of the produced MIP layers is to calculate a parameter called the imprinting factor (*IF*) [32,33]. *IF* is generally evaluated according to equation (2):

$$IF = \frac{Q_{\mathrm{MIP}}}{Q_{\mathrm{NIP}}} \quad (2)$$

where Q_{MIP} – is the equilibrium binding capacity of MIP; Q_{NIP} – is the equilibrium binding capacity of NIP.

However, in general, using equation (2), *IF* is calculated from chromatography or piezo-microgravimetry measurements. Ayerdurai et al., [34] recommend the use of the term *apparent imprinting factor* (*AIF*) if it is determined by comparing the MIP and NIP signals using a technique other than piezo-microgravimetry. Generally, in electrochemical measurements, *IF* is calculated by comparing the ratio between the slopes of MIP and of NIP [35–37], or the selected signal response ratio of MIP and NIP [38]. In this study, the *AIF* was calculated as the ratio of the relative decrease in the current – $\Delta I_{\%}$ of MIP and NIP films, according to equation (3):

$$AIF = \frac{\Delta I_{\%(\mathrm{MIP})}}{\Delta I_{\%(\mathrm{NIP})}} \quad (3)$$

where $\Delta I_{\%(\mathrm{MIP})}$ – the relative decrease in the current of MIP, %; $\Delta I_{\%(\mathrm{NIP})}$ – the relative decrease in the current of NIP, %.

The differences in a relative current's decrease of MIP and NIP layers after the interaction with melamine (1 μM) are demonstrated in Fig. 2B. The *AIF* value is displayed above the columns. The *AIF* of prepared MIP layers was 1.59. An additional drop of the peak oxidation current for MIP could have been caused by stronger specific interactions with melamine, in comparison to NIP, which only interacted with melamine non-specifically. Therefore, Ppy was successfully imprinted with melamine templates and the obtained layer can be used for further design of melamine sensor systems. However, the imprinting factor value of 1.59 of the MIP layer is quite low. Guan et al., [39] study described that the higher *AIF* correlates with the better uptake of template molecules and the higher specificity of the template. Low *AIF* can be attributed to low specificity, high non-specific interactions, or to both mentioned effects. These observations of low *AIF* were also explored in the research by Giulio et al., [40] and Turco et al., [41]. Therefore, MIPs have to be further improved. Thus, in this study, MIPs were modified by incorporating AuNPs or gold(I) complexes.

In the subsequent research, the addition of AuNPs or gold(I) complexes in the polymerization solution was studied. In previous studies, these compounds were applied to increase the electrocatalytic properties of the polymer layers [17,19,42–47]. Generally, the size of AuNPs was determined using atomic force microscopy (AFM). The methodology of the AuNPs synthesis and characterization was reported by German et al., [19,28] and later by Brasiunas et al., [48] study. The used method for the synthesis of AuNPs has shown great reproducibility and precise size control of the AuNPs. The surface morphology of the polymer films was studied using a scanning electron microscope (SEM). SEM images with different magnifications are provided in the supplementary material (Fig. 1S-4S). No morphological differences between NIP and MIP, and non-modified and AuNPs-modified Ppy were observed. Moreover, AuNPs in the Ppy were not visible using SEM due to several reasons. One of them was the limitations of the SEM device used in this work as nanoparticles were too small to be detected within the composite. Second, the globular structure of Ppy hindered the focus and imaging process. Lastly, the Ppy was constantly melting at the magnifications of × 300 k and higher, thus resulting in distorted and blurry SEM images. Formed MIP and NIP composites with nanomaterials were

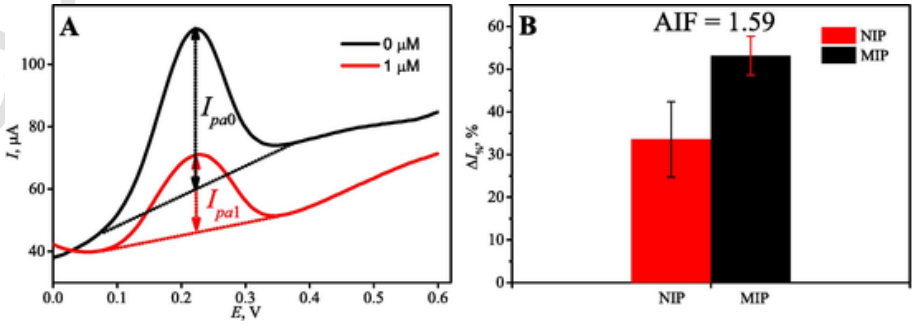

Fig. 2. A) DPV measurements of the MIP layer after the incubation in PBS with 0 M melamine and 1 μM melamine. The dotted line displays the method of extracting the analytical signal from these curves. **B)** The differences in a relative decrease in the current of MIP and NIP after the incubation with 1 μM melamine. *AIF* in the graph represents the signal ratio calculated according to equation (3). Error bars in the graph represent the standard deviation of this data set (n = 3).

analyzed in the same conditions as non-modified MIP and NIP layers. Modifications of these polymer layers aim to obtain a film where the DPV response of MIP to melamine was greater, and the *AIF* was as high as possible. The differences in a relative decrease in the current after the interaction with melamine of AuNPs-modified polymers are depicted in Fig. 3A-C. Fig. 3A illustrates the effect of modification with 3.5 nm diameter AuNPs. As AuNP concentration was increased, the oxidation peak current decreased. The highest *AIF* value was observed when the polymerization was carried out from a solution containing 0.05 nM of 3.5 nm AuNPs. In these conditions, the observed *AIF* of MIP was 6.61. Fig. 3B demonstrates a change in electrochemical signal owing to the modification of polymers with 6 nm AuNPs. Here, MIP synthesized from a solution containing 0.1 nM 6 nm AuNPs had the best features. The monitored *AIF* was 1.86. The evaluation of MIP and NIP prepared from a solution with 13 nm AuNPs is presented in Fig. 3C. Both NIP and MIP exhibited a significantly greater response to melamine. However, the *AIF* in these conditions was notably lower than that with 3.5 nm and 6 nm AuNPs. In these conditions, the highest *AIF* was 1.18 and was observed when the layers were prepared from a mixture with 0.01 nM 13 nm AuNPs. In this experiment, AuNPs could have affected polymers in two ways. Owing to the great surface-to-volume ratio of AuNPs and their electrocatalytic properties [19,20], the registered current should increase and the sensor should be more susceptible to the change in surface concentration of electrochemically active substances, in this case – $K_3[Fe(CN)_6]/K_4[Fe(CN)_6]$ redox probe. On the other hand, it was reported that AuNPs can interact with amine groups [21]. In this work, AuNPs were covered with citrate molecules [28], therefore the surface of AuNPs was covered with the carboxylic groups, which can non-specifically interact with melamine, making MIP and NIP composites more sensitive toward melamine molecules.

The following experiments observed the changes due to the modification of MIP and NIP with other materials – gold(I) complexes. Fig. 3D illustrates the obtained results of the layers that were modified with 1 μM of gold(I) complexes **1**, **2**, and **3**. The polymerization was performed from a solution with gold(I) complexes. The effect of gold(I) complexes **1**, **2**, and **3 on AIF** was insufficient for further application as electrochemical MIP sensors for melamine.

Traditionally, gold(I) complexes are used in medicine for their antirheumatic [49], anticancer [50], or anti-infective effects, and there is currently extensive research for other therapeutic applications [51]. At the time of this paper, there are no previously reported studies on the electrocatalytic properties of gold(I) complexes as it was examined in this study. In general, gold nanostructures exhibit electrocatalytic properties. One aim of this part of the study was to determine whether these gold(I) complexes were also electrocatalytic. However, it is difficult to affirm what effect was observed from these results and further studies are required to assess it.

The MIP-based sensors obtained from a polymerization solution consisting of 50 mM pyrrole, 5 mM melamine, and 0.05 nM 3.5 nm AuNPs, demonstrated the most appealing characteristics. Therefore, further experiments were performed using MIP and NIP prepared at these conditions. It was noticed that not only MIP and NIP layer interactions with melamine affected the strength of the signal measured by DPV. The electrochemical evaluation itself may have been somewhat destructive to the polymers. The Ppy could be slightly oxidized during each measurement [52], therefore, the analytic signals were slightly distorted. To minimize the plausible effect of altering the polymeric layer of Ppy during the study, it was decided to overoxidize MIP and NIP before evaluating interactions with melamine. Overoxidation of MIP and NIP was carried out by CV (10 potential scans) in 0.1 M NaOH solution, in the potential range from + 0.8 V to + 1.2 V *vs* $Ag/AgCl_{(3M\ KCl)}$.

The manufactured MIP and NIP films were characterized using the DPV in the following part of the research. Before each electrochemical characterization, polymers were incubated for 10 min in PBS solutions with varying concentrations of melamine: 0 nM, 1 nM, 5 nM, 10 nM, 50 nM, 0.1 μM, 0.5 μM, 1 μM, and 5 μM. The voltammograms obtained by the DPV for MIP layers are presented in Fig. 4A. It was noted that with the increase of melamine concentration during the incubation, the oxidation peak area and height measured by the DPV decreased for both Ppy films. The peak anodic current maximum was recorded at 0.222 V *vs* $Ag/AgCl_{(3M\ KCl)}$. Oxidation peak height (I_{pa}) values were obtained, and the calibration curve (peak height dependence on the melamine concentration) is illustrated in Fig. 4B. The difference in oxi-

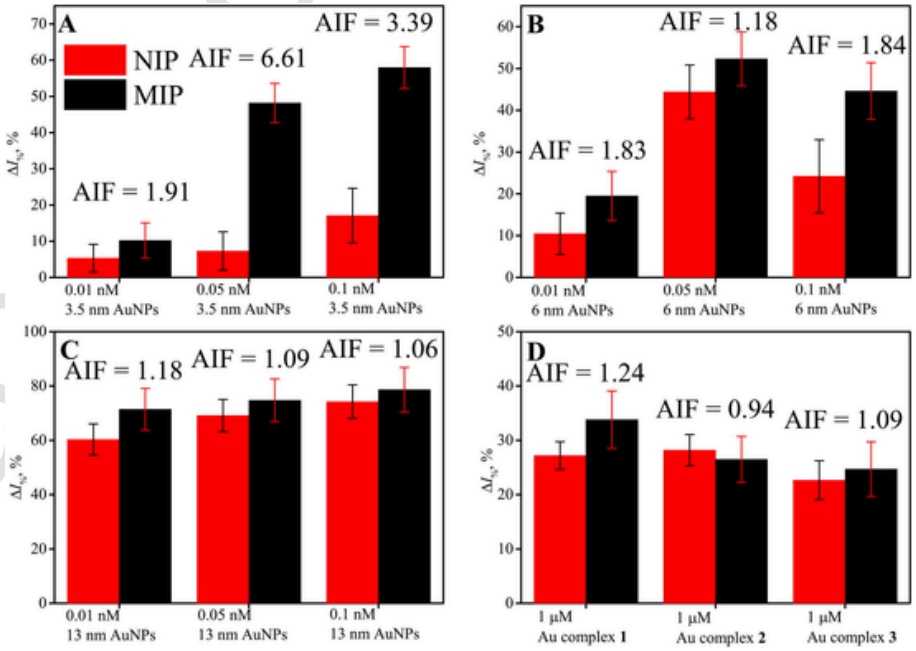

Fig. 3. The differences in a relative decrease in the current of MIP and NIP after the incubation with 1 μM melamine, when MIP and NIP were prepared from a solution containing: **A)** 0.01 nM, 0.05 nM, or 0.1 nM 3.5 nm diameter AuNPs; **B)** 0.01 nM, 0.05 nM, or 0.1 nM 6 nm diameter AuNPs; **C)** 0.01 nM; 0.05 nM, or 0.1 nM 13 nm diameter AuNPs; **D)** 1 μM gold(I) complexes **1**, **2**, or **3**. The *AIF* in the graph represents the signal ratios calculated according to equation (3). Error bars in the graph represent the standard deviation of these data sets (n = 3).

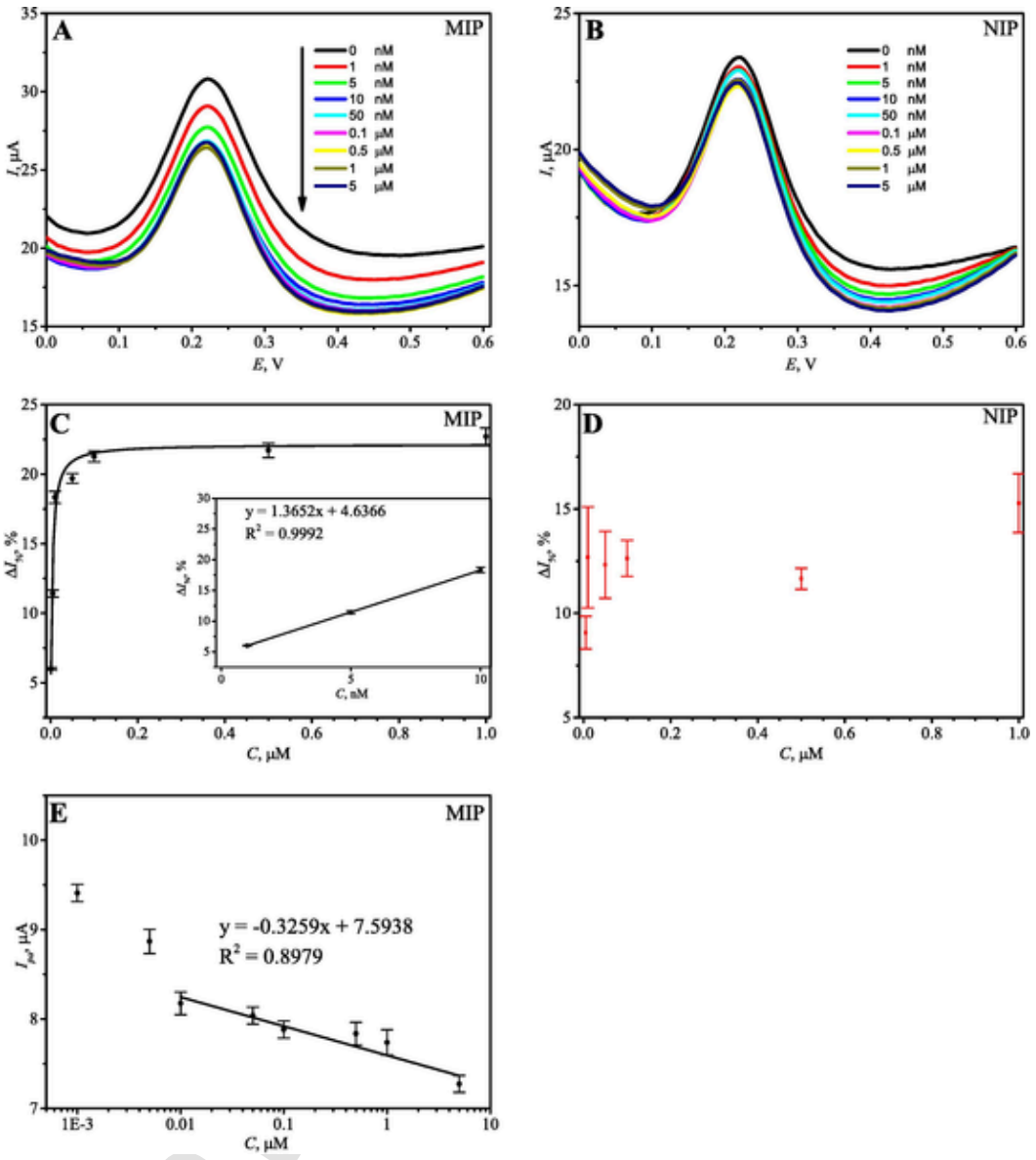

Fig. 4. DPV method-based evaluation of melamine interaction with MIP or NIP. DPV measurements after the incubation in PBS with varying concentrations of melamine for **A)** the MIP layer; and **B)** the NIP layer. **C)** The decrease of oxidation current peak height of MIP due to the increase in the concentration of melamine. **C(inset)** – The decrease of oxidation current peak height of MIP due to the increase in the concentration of melamine, in the interval of lower concentrations. The slope of the displayed linear equation and the displayed linear equation were used for further calculations. **D)** The decrease of oxidation current peak height of NIP due to the increase in the concentration of melamine. **E)** the dependence of MIP oxidation current peak height on the concentration of melamine, displayed in a logarithmic scale. Error bars in the graph represent the standard deviation of this data set (n = 3).

dation current was owing to the increasing concentration of melamine. MIP layers interacted with melamine molecules due to the additional specific interactions. Therefore, as melamine concentration on the surface of the MIP increased, the measured oxidation current decreased due to the hindrance of electron pathways [30].

The oxidation peak current changes were followed in presence of increasing of melamine concentrations from 1 nM to 5 μM. The decrease of peak oxidation current ($\Delta I_{\%}$) dependence on the concentration of melamine is illustrated in Fig. 4C. For better comprehension, dependence at the lower melamine concentration in the range from 1 nM to 10 nM was presented in Fig. 4C (inset). After incubating MIP in a solution with 1 nM of melamine, the oxidation current decreased by 6.01 ± 0.09 %.

$$\Delta I_{\%} = \Delta I_{\%,max} \times \frac{K \times c}{1 + K \times c} \quad (4)$$

where $\Delta I_{\%,\ max}$ –the normalized DPV peak current value, %; K – the Langmuir constant, μM⁻¹; c – the concentration of melamine, μM.

Jyoti et al., [35] adapted the Langmuir isotherm equation for the electrochemical measurements of MIPs in their research. In our study, the curve in Fig. 4C was fitted according to the analogous Langmuir isotherm expression, which is presented in equation (4). The application of this equation yielded the normalized DPV peak current value, which was equal to 22.14 ± 1.26 %, and the Langmuir constant, which was equal to 343.85 ± 53.47 μM⁻¹. Unfortunately, the data of NIP, presented in Fig. 4D, did not follow this or any particular dependence, thus, MIP and NIP parameters for this expression could not be compared. $\Delta I_{\%}$ was calculated using equation (4):

LOD and limit of quantification (LOQ) for MIP were estimated by equations (5) and (6):

$$\mathrm{LOD} = \frac{3.3\sigma}{S} \quad (5)$$

$$\mathrm{LOQ} = \frac{10\sigma}{S} \quad (6)$$

where σ – is the standard deviation of the response measured in 0 nM concentration of melamine; S – is the slope of the calibration curve.

LOD for MIP was estimated by equation (5) and was equal to 0.83 nM of melamine and the LOQ was calculated by equation (6) and was 2.50 nM of melamine. LOD for MIP was comparable to other MIP-based sensors for the detection of melamine described in other studies.

The outbreak of acute renal failure in house pets linked to melamine-contaminated pet foods induced the research of melamine [11,12,61]. There are more studies employing electrochemical methods and MIPs for the detection of melamine [8,24–26,62] but the summary presented in Table 2 overviews only the latest MIP-based electrochemical sensors published in the period from 2018 to 2022. The basis of the described sensor recognition elements is MIPs. The sensing of melamine was usually executed electrochemically by indirect means using $[Fe(CN)_6]^{3-/4-}$ as a redox probe by applying DPV [22,53] just like in this paper, or EIS [54–56,59]. The developed sensors were also implemented in the determination of melamine in real samples (milk or infant formula). The authors state that these results were satisfactory and sensors can be employed in the analysis of real samples.

4. Conclusions

The graphite rod electrode surface was modified with melamine-imprinted polymer (MIP) and non-imprinted polymer (NIP) layers. Additional modifications with 3.5 nm, 6 nm, and 13 nm diameter AuNPs, or gold(I) complexes **1**, **2,** and **3** were evaluated. DPV was selected for the analysis and the monitoring of the decrease of peak oxidation current after the incubation of MIP and NIP in 1 μM melamine was evaluated. The optimum outcomes were achieved when the polymerization of MIP was conducted using a solution containing 50 mM pyrrole, 5 mM melamine, and 0.05 nM AuNPs with a diameter of 3.5 nm. Under these precise conditions, *AIF* MIP towards melamine was 6.61. The detection of melamine was further characterized using overoxidized MIP and NIP. Using MIP the LOD was estimated at 0.83 nM of melamine. The observed LOD is comparable to other MIP-based systems for the detection of melamine reported in other studies.

CRediT authorship contribution statement

Ernestas Brazys: Conceptualization, Data curation, Formal analysis, Methodology, Visualization, Writing – original draft. **Vilma Ratautaite:** Data curation, Formal analysis, Writing – original draft. **Benediktas Brasiunas:** Data curation, Formal analysis. **Almira Ramanaviciene:** Conceptualization, Writing – review & editing. **Laura Rodríguez:** Funding acquisition, Writing – review & editing. **Andrea Pinto:** Data curation. **Demetrio Milea:** Data curation, Funding acquisition. **Urte Prentice:** Data curation, Writing – review & editing. **Arunas Ramanavicius:** Conceptualization, Data curation, Funding acquisition, Supervision, Writing – review & editing.

Declaration of competing interest

The authors declare that they have no known competing financial interests or personal relationships that could have appeared to influence the work reported in this paper.

Data availability

Data will be made available on request.

Table 2
Characteristics of electrochemical sensors for melamine detection.

Electrode	Modification of electrode with MIPs	Methods	LOD and linear range	Comments about samples	Ref.
MIL-53(Fe)[1]-modified GCE[2]	Poly(methacrylic acid)	DPV	8.21×10^{-12} M 10^{-11} M – 10^{-6} M	Milk samples	[53]
AuNPs and melamine-aptamer modified GCE	Polydopamine	DPV	6.7×10^{-13} M 10^{-12} M – 10^{-4} M	Milk samples	[22]
GO[3] modified GCE	Polypyrrole	EIS[4]	8.3×10^{-10} M 4.0×10^{-9} M – 2.4×10^{-7} M	Milk samples	[54]
GCE	Poly(aniline-co-acrylic acid)	DPV	1.72×10^{-11} M, 1×10^{-10}— 1.8×10^{-7} nM	Infant formula and raw milk	[23]
GCE	Polyaniline	SWV[5]	4.47×10^{-10} M 6.0×10^{-10} M – 1.6×10^{-8} M	Infant formula	[55]
GCE	Poly (aniline-co-itaconic acid)	SWV	1.79×10^{-11} M 2.5×10^{-10} M – 1.0×10^{-7} M	Infant formula or raw milk	[56]
MWCNTs[6] modified GCE	Poly(acrylic acid-co-(7-(4-vinylbenzyloxy)-4-methyl coumarin)–co-ethylhexyl acrylate)	DPV	5.6×10^{-13} M 1.0×10^{-12} M – 1.0×10^{-6} M	Milk samples	[57]
Pt	Ppy on GO-Fe_3O_4@SiO_2 nanocomposite	CV	$2.8\ 10^{-9}$ M 5.0×10^{-7} – 1.0×10^{-5} M	Milk, yoghurt, cheese, and dough samples	[58]
SAM[7]-modified Gold-coated silicon wafer	Siloxane	SWV	0.4×10^{-9} M 5×10^{-9} M – 10^{-6} M	–	[59]
Gold QCM[8] electrode	Poly(methacrylic acid)	QCM	1.8×10^{-8} M 4.0×10^{-7} M – 7.9×10^{-6} M	Milk samples	[60]
Graphite electrode	Polypyrrole decorated with 3.5 nm AuNPs	DPV	8.3×10^{-10} M	–	This work

[1] MIL-53(Fe) – iron metal–organic framework described in [53]; [2]GCE – glassy carbon electrode; [3]GO – graphene oxide; [4]EIS – electrochemical impedance spectroscopy; [5]SWV – square wave voltammetry; [6]MWCNTs – multi-walled carbon nanotubes; [7]SAM – self-assembled monolayer; [8]QCM – quartz crystal microbalance.

Acknowledgments

The authors are grateful to projects PID2019-104121 GB-I00 funded by the Ministerio de Ciencia e Innovación of Spain MCIN/AEI/10.13039/501100011033.

This publication is also based upon work from European Cooperation in Science and Technology (COST) Action CA18202 – NECTAR – Network for Equilibria and Chemical Thermodynamics Advanced Research, supported by COST (European Cooperation in Science and Technology).

Appendix A. Supplementary data

Supplementary data to this article can be found online at https://doi.org/10.1016/j.microc.2024.109890.

References

[1] A.K.-C. Hau, T.H. Kwan, P.K.-t. Li, Melamine toxicity and the kidney, Journal of the American Society of Nephrology, 20(2009) 245-50. https://doi.org/10.1681/ASN.2008101065.

[2] R.P. Dalal, D.S. Goldfarb, Melamine-related kidney stones and renal toxicity, Nat. Rev. Nephrol. 7 (2011) 267–274, https://doi.org/10.1038/nrneph.2011.24.

[3] Q. Li, P. Song, J. Wen, Melamine and food safety: a 10-year review, Current Opinion in Food Science 30 (2019) 79–84, https://doi.org/10.1016/j.cofs.2019.05.008.

[4] L. Zhang, L.-L. Wu, Y.-P. Wang, A.-M. Liu, C.-C. Zou, Z.-Y. Zhao, Melamine-contaminated milk products induced urinary tract calculi in children, World J. Pediatr. 5 (2009) 31–35, https://doi.org/10.1007/s12519-009-0005-6.

[5] Y. Lu, Y. Xia, G. Liu, M. Pan, M. Li, N.A. Lee, et al., A review of methods for detecting melamine in food samples, Crit Rev Anal Chem 47 (2017) 51–66, https://doi.org/10.1080/10408347.2016.1176889.

[6] Q. Cao, H. Zhao, Y. He, X. Li, L. Zeng, N. Ding, et al., Hydrogen-bonding-induced colorimetric detection of melamine by nonaggregation-based Au-NPs as a probe, Biosens. Bioelectron. 25 (2010) 2680–2685, https://doi.org/10.1016/j.bios.2010.04.046.

[7] Q. Cao, H. Zhao, Y. He, N. Ding, J. Wang, Electrochemical sensing of melamine with 3,4-dihydroxyphenylacetic acid as recognition element, Anal. Chim. Acta 675 (2010) 24–28, https://doi.org/10.1016/j.aca.2010.07.002.

[8] A. Pietrzyk, W. Kutner, R. Chitta, M.E. Zandler, F. D'Souza, F. Sannicolò, et al., Melamine acoustic chemosensor based on molecularly imprinted polymer film, Anal Chem 81 (2009) 10061–10070, https://doi.org/10.1021/ac9020352.

[9] F. Wang, L. Zhu, J. Zhang, Electrochemical sensor for levofloxacin based on molecularly imprinted polypyrrole–graphene–gold nanoparticles modified electrode, Sens Actuat B-Chem 192 (2014) 642–647, https://doi.org/10.1016/j.snb.2013.11.037.

[10] G. Vasapollo, R.D. Sole, L. Mergola, M.R. Lazzoi, A. Scardino, S. Scorrano, et al., Molecularly imprinted polymers: present and future prospective, Int J Mol Sci 12 (2011) 5908–5945, https://doi.org/10.3390/ijms12095908.

[11] K. Rovina, S. Siddiquee, A review of recent advances in melamine detection techniques, J. Food Compos. Anal. 43 (2015) 25–38, https://doi.org/10.1016/j.jfca.2015.04.008.

[12] C.F. Nascimento, P.M. Santos, E.R. Pereira-Filho, F.R.P. Rocha, Recent advances on determination of milk adulterants, Food Chem 221 (2017) 1232–1244, https://doi.org/10.1016/j.foodchem.2016.11.034.

[13] J.J. BelBruno, Molecularly imprinted polymers, Chem. Rev. 119 (2019) 94–119, https://doi.org/10.1021/acs.chemrev.8b00171.

[14] A.A. Lahcen, A. Amine, Recent advances in electrochemical sensors based on molecularly imprinted polymers and nanomaterials, Electroanalysis 31 (2019) 188–201, https://doi.org/10.1002/elan.201800623.

[15] A. Jahanban-Esfahlan, L. Roufegarinejad, R. Jahanban-Esfahlan, M. Tabibiazar, R. Amarowicz, Latest developments in the detection and separation of bovine serum albumin using molecularly imprinted polymers, Talanta 207 (2020) 120317, https://doi.org/10.1016/j.talanta.2019.120317.

[16] M. Majdinasab, M. Daneshi, J. Louis Marty, Recent developments in non-enzymatic (bio)sensors for detection of pesticide residues: Focusing on antibody, aptamer and molecularly imprinted polymer, Talanta, 232(2021) 122397. https://doi.org/10.1016/j.talanta.2021.122397.

[17] H. Essousi, H. Barhoumi, S. Karastogianni, S.T. Girousi, An electrochemical sensor based on reduced graphene oxide, gold nanoparticles and molecular imprinted over-oxidized polypyrrole for amoxicillin determination, Electroanalysis 32 (2020) 1546–1558, https://doi.org/10.1002/elan.201900751.

[18] J. Gu, H. Dai, Y. Kong, Y. Tao, H. Chu, Z. Tong, Chiral electrochemical recognition of cysteine enantiomers with molecularly imprinted overoxidized polypyrrole-Au nanoparticles, Synth. Met. 222 (2016) 137–143, https://doi.org/10.1016/j.synthmet.2016.05.007.

[19] N. German, A. Ramanavicius, J. Voronovic, A. Ramanaviciene, Glucose biosensor based on glucose oxidase and gold nanoparticles of different sizes covered by polypyrrole layer, Colloid Surface A 413 (2012) 224–230, https://doi.org/10.1016/j.colsurfa.2012.02.012.

[20] S. Kumar, I. Jha, N.K. Mogha, P. Venkatesu, Biocompatibility of surface-modified gold nanoparticles towards red blood cells and haemoglobin, Appl. Surf. Sci. 512 (2020) 145573, https://doi.org/10.1016/j.apsusc.2020.145573.

[21] N. Elahi, M. Kamali, M.H. Baghersad, Recent biomedical applications of gold nanoparticles: a review, Talanta 184 (2018) 537–556, https://doi.org/10.1016/j.talanta.2018.02.088.

[22] C. Yu, L. Li, Y. Ding, H. Liu, H. Cui, F. Zhang, et al., A sensitive molecularly imprinted electrochemical aptasensor for highly specific determination of melamine, Food Chem. 363 (2021) 130202, https://doi.org/10.1016/j.foodchem.2021.130202.

[23] M.B. Regasa, T. Refera Soreta, O.E. Femi, P. C. Ramamurthy, Development of molecularly imprinted conducting polymer composite film-based electrochemical sensor for melamine detection in infant formula, ACS Omega, 5(2020) 4090-9. https://doi.org/10.1021/acsomega.9b03747.

[24] R. Liang, R. Zhang, W. Qin, Potentiometric sensor based on molecularly imprinted polymer for determination of melamine in milk, Sens Actuat. B-Chem. 141 (2009) 544–550, https://doi.org/10.1016/j.snb.2009.05.024.

[25] B. Wu, Z. Wang, D. Zhao, X. Lu, A novel molecularly imprinted impedimetric sensor for melamine determination, Talanta 101 (2012) 374–381, https://doi.org/10.1016/j.talanta.2012.09.044.

[26] Y.T. Liu, J. Deng, X.L. Xiao, L. Ding, Y.L. Yuan, H. Li, et al., Electrochemical sensor based on a poly(para-aminobenzoic acid) film modified glassy carbon electrode for the determination of melamine in milk, Electrochim. Acta 56 (2011) 4595–4602, https://doi.org/10.1016/j.electacta.2011.02.088.

[27] V. Ratautaite, E. Brazys, A. Ramanaviciene, A. Ramanavicius, Electrochemical sensors based on L-tryptophan molecularly imprinted polypyrrole and polyaniline, J. Electroanal. Chem. 917 (2022) 116389, https://doi.org/10.1016/j.jelechem.2022.116389.

[28] N. German, A. Ramanaviciene, J. Voronovic, A. Ramanavicius, Glucose biosensor based on graphite electrodes modified with glucose oxidase and colloidal gold nanoparticles, Microchim. Acta 168 (2010) 221–229, https://doi.org/10.1007/s00604-009-0270-z.

[29] A. Pinto, M. Echeverri, B. Gómez-Lor, L. Rodríguez, Highly emissive supramolecular gold(i)–BTD materials, Dalton Trans. 51 (2022) 8340–8349, https://doi.org/10.1039/D2DT00950A.

[30] Q. Cao, H. Zhao, L. Zeng, J. Wang, R. Wang, X. Qiu, et al., Electrochemical determination of melamine using oligonucleotides modified gold electrodes, Talanta 80 (2009) 484–488, https://doi.org/10.1016/j.talanta.2009.07.006.

[31] K. Haupt, Molecularly imprinted polymers: the next generation, Anal Chem, 75 (2003) 376 A-83 A. https://doi.org/10.1021/ac031385h.

[32] E.N. Ndunda, Molecularly imprinted polymers—a closer look at the control polymer used in determining the imprinting effect: a mini review, J. Mol. Recognit. 33 (2020) e2855.

[33] V. Ratautaite, U. Samukaite-Bubniene, D. Plausinaitis, R. Boguzaite, D. Balciunas, A. Ramanaviciene, et al., Molecular imprinting technology for determination of uric acid, Int J Mol Sci 22 (2021) 5032, https://doi.org/10.3390/ijms22095032.

[34] V. Ayerdurai, M. Cieplak, W. Kutner, Molecularly imprinted polymer-based electrochemical sensors for food contaminants determination, TRAC-Trends Anal Chem 158 (2023) 116830, https://doi.org/10.1016/j.trac.2022.116830.

[35] Jyoti, C. Gonzato, T. Żołek, D. Maciejewska, A. Kutner, F. Merlier, et al., Molecularly imprinted polymer nanoparticles-based electrochemical chemosensors for selective determination of cilostazol and its pharmacologically active primary metabolite in human plasma, Biosensors and Bioelectronics, 193(2021) 113542. https://doi.org/10.1016/j.bios.2021.113542.

[36] H. Munawar, J.S. Mankar, M.D. Sharma, A. Garcia-Cruz, L.A.L. Fernandes, M. Peacock, et al., Highly selective electrochemical nanofilm sensor for detection of carcinogenic PAHs in environmental samples, Talanta 219 (2020) 121273, https://doi.org/10.1016/j.talanta.2020.121273.

[37] F. Zouaoui, S. Bourouina-Bacha, M. Bourouina, I. Abroa-Nemeir, H. Ben Halima, J. Gallardo-Gonzalez, et al., Electrochemical impedance spectroscopy determination of glyphosate using a molecularly imprinted chitosan, Sens Actuat B-Chem, 309(2020) 127753. https://doi.org/10.1016/j.snb.2020.127753.

[38] A.F.T. Waffo, C. Yesildag, G. Caserta, S. Katz, I. Zebger, M.C. Lensen, et al., Fully electrochemical MIP sensor for artemisinin, Sens Actuat. B-Chem. 275 (2018) 163–173, https://doi.org/10.1016/j.snb.2018.08.018.

[39] G. Guan, S. Wang, H. Zhou, K. Zhang, R. Liu, Q. Mei, et al., Molecularly imprinted polypyrrole nanonecklaces for detection of herbicide through molecular recognition-amplifying current response, Anal. Chim. Acta 702 (2011) 239–246, https://doi.org/10.1016/j.aca.2011.06.047.

[40] T. Di Giulio, E. Mazzotta, C. Malitesta, Molecularly imprinted polyscopoletin for the electrochemical detection of the chronic disease marker lysozyme, Biosensors 11 (2021) 3, https://doi.org/10.3390/bios11010003.

[41] A. Turco, S. Corvaglia, E. Mazzotta, Electrochemical sensor for sulfadimethoxine based on molecularly imprinted polypyrrole: Study of imprinting parameters, Biosens. Bioelectron. 63 (2015) 240–247, https://doi.org/10.1016/j.bios.2014.07.045.

[42] N. German, A. Ramanaviciene, A. Ramanavicius, Formation of polyaniline and polypyrrole nanocomposites with embedded glucose oxidase and gold nanoparticles, Polymers (basel) 11 (2019) 377, https://doi.org/10.3390/polym11020377.

[43] N. German, A. Popov, A. Ramanaviciene, A. Ramanavicius, Formation and electrochemical characterisation of enzyme-assisted formation of polypyrrole and polyaniline nanocomposites with embedded glucose oxidase and gold nanoparticles, J. Electrochem. Soc. 167 (2020) 165501, https://doi.org/10.1149/1945-7111/abc9dc.

[44] L. Devkota, L.T. Nguyen, T.T. Vu, B. Piro, Electrochemical determination of tetracycline using AuNP-coated molecularly imprinted overoxidized polypyrrole sensing interface, Electrochim. Acta 270 (2018) 535–542, https://doi.org/10.1016/j.electacta.2018.03.104.

[45] M.A. Alonso-Lomillo, O. Domínguez-Renedo, Molecularly imprinted polypyrrole based electrochemical sensor for selective determination of ethanethiol, Talanta 253 (2023) 123936, https://doi.org/10.1016/j.talanta.2022.123936.

[46] M. Wu, X. Wang, J. Shan, H. Zhou, Y. Shi, M. Li, et al., Sensitive and selective electrochemical sensor based on molecularly imprinted polypyrrole hybrid nanocomposites for tetrabromobisphenol A detection, Anal. Lett. 52 (2019) 2506–2523, https://doi.org/10.1080/00032719.2019.1617298.
[47] Y. Xu, Z. Gao, W. Chen, E. Wang, Y. Li, Preparation and application of malachite green molecularly imprinted/gold nanoparticle composite film–modified glassy carbon electrode, Ionics 25 (2019) 1177–1185, https://doi.org/10.1007/s11581-018-2778-x.
[48] B. Brasiunas, A. Popov, A. Ramanavicius, A. Ramanaviciene, Gold nanoparticle based colorimetric sensing strategy for the determination of reducing sugars, Food Chem. 351 (2021) 129238, https://doi.org/10.1016/j.foodchem.2021.129238.
[49] G.G. Graham, M.W. Whitehouse, G.R. Bushell, Aurocyanide, dicyano-aurate (I), a pharmacologically active metabolite of medicinal gold complexes, Inflammopharmacology 16 (2008) 126–132, https://doi.org/10.1007/s10787-007-0020-y.
[50] I. Kostova, P. Bentham Science, Gold coordination complexes as anticancer agents, Anti-Cancer Agents in Medicinal Chemistry, 6(2006) 19-32. http://doi.org/10.2174/187152006774755500.
[51] M. Gil-Moles, U. Basu, R. Büssing, H. Hoffmeister, S. Türck, A. Varchmin, et al., Gold metallodrugs to target coronavirus proteins: inhibitory effects on the spike-ACE2 interaction and on PLpro Protease activity by auranofin and gold organometallics**, Chemistry – A European Journal, 26(2020) 15140-4. https://doi.org/10.1002/chem.202004112.
[52] K. Maksymiuk, Chemical reactivity of polypyrrole and its relevance to polypyrrole based electrochemical sensors, Electroanalysis 18 (2006) 1537–1551, https://doi.org/10.1002/elan.200603573.
[53] J. An, L. Li, Y. Ding, W. Hu, D. Duan, H. Lu, et al., A novel molecularly imprinted electrochemical sensor based on Prussian blue analogue generated by iron metal organic frameworks for highly sensitive detection of melamine, Electrochim. Acta 326 (2019) 134946, https://doi.org/10.1016/j.electacta.2019.134946.
[54] M. Shamsipur, N. Moradi, A. Pashabadi, Coupled electrochemical-chemical procedure used in construction of molecularly imprinted polymer-based electrode: a highly sensitive impedimetric melamine sensor, J. Solid State Electrochem. 22 (2018) 169–180, https://doi.org/10.1007/s10008-017-3731-z.
[55] M.B. Regasa, T.R. Soreta, O.E. Femi, P.C. Ramamurthy, S. Kumar, Molecularly imprinted polyaniline molecular receptor–based chemical sensor for the electrochemical determination of melamine, J. Mol. Recognit. 33 (2020) e2836.
[56] M.B. Regasa, T.R. Soreta, O.E. Femi, P.C. Ramamurthy, S. Subbiahraj, Novel multifunctional molecular recognition elements based on molecularly imprinted poly (aniline-co-itaconic acid) composite thin film for melamine electrochemical detection, Sens. Bio-Sens. Res. 27 (2020) 100318, https://doi.org/10.1016/j.sbsr.2019.100318.
[57] S. Xu, G. Lin, W. Zhao, Q. Wu, J. Luo, W. Wei, et al., Necklace-like molecularly imprinted nanohybrids based on polymeric nanoparticles decorated multiwalled carbon nanotubes for highly sensitive and selective melamine detection, ACS Appl. Mater. Interfaces 10 (2018) 24850–24859, https://doi.org/10.1021/acsami.8b08558.
[58] M. Biabani, A. Nezhadali, A. Nakhaei, H. Nakhaei, Melamine recognition: molecularly imprinted polymer for selective and sensitive determination of melamine in food samples, Int. J. Anal. Chem. 2020 (2020) 8864144, https://doi.org/10.1155/2020/8864144.
[59] M. Bengamra, N. Grayaa-Jaoued, A. Khlifi-Riani, M.M. Chehimi, R. Kalfat, Highly selective molecularly imprinted sol-gel membrane grafted to gold for the detection of melamine, Silicon 11 (2019) 2267–2274, https://doi.org/10.1007/s12633-017-9674-2.
[60] Ş. Ceylan Cömert, E. Özgür, L. Uzun, M. Odabaşı, The creation of selective imprinted cavities on quartz crystal microbalance electrode for the detection of melamine in milk sample, Food Chem, 372(2022) 131254. https://doi.org/10.1016/j.foodchem.2021.131254.
[61] F. Sun, W. Ma, L. Xu, Y. Zhu, L. Liu, C. Peng, et al., Analytical methods and recent developments in the detection of melamine, TRAC-Trends Anal. Chem. 29 (2010) 1239–1249, https://doi.org/10.1016/j.trac.2010.06.011.
[62] H. Rao, M. Chen, H. Ge, Z. Lu, X. Liu, P. Zou, et al., A novel electrochemical sensor based on Au@PANI composites film modified glassy carbon electrode binding molecular imprinting technique for the determination of melamine, Biosens. Bioelectron. 87 (2017) 1029–1035, https://doi.org/10.1016/j.bios.2016.09.074.